Study of isothermal δ' (Al$_3$Li) precipitation in an Al–Li alloy by thermoelectric power

I. Gutiérrez-Urrutia

Abstract We study the isothermal δ' (Al$_3$Li) precipitation kinetics in an Al–2.3 wt% Li–0.1 wt% Zr alloy by means of the measurement of the thermoelectric power (TEP) in the temperature range between 120 and 180 °C. We obtain that the nucleation-and-growth stage of δ' precipitation reaction can be well described by the Johnson–Mehl–Avrami–Kolmogorov (JMAK) relation. This result suggests that the JMAK relation provides a good description of the impingement effect of growing δ' precipitates where interactions mainly occur on neighbouring precipitates. The activation energy associated to the nucleation-and-growth stage calculated from the JMAK fit is 52 ± 1 kJ/mol. The small activation energy obtained is ascribed to the presence of a large amount of excess vacancies quenched-in from the ageing temperature, inherent to the experimental conditions of the measurement of the TEP, reducing the activation energy to a value close to the vacancy migration energy in aluminium (45–65 kJ/mol). The Avrami exponent of this stage ranges between 1.5 and 1.65. These kinetic parameters indicate that δ' particles grow via a three-dimensional vacancy migration-controlled mechanism.

Introduction

Aluminium–lithium alloys have received a great deal of attention over the past years as structural materials in aerospace applications because of their low specific density (unit addition of lithium to aluminium lowers the density by approximately 3% and increases the modulus by approximately 6%) combined with superior stiffness and strength than conventional aluminium alloys [1–3]. The addition of lithium promotes the precipitation of the metastable and ordered δ' phase (Al$_3$Li, L1$_2$ structure) and the equilibrium Al–Li phase (δ-AlLi, b.c.c. structure). The δ' particles are fully coherent with the matrix conferring high strength because of order strengthening [1, 4] whereas δ phase mainly precipitates at grain boundaries [5]. Latest generation of Al–Li alloys (2198, 2196, 2050) includes the addition of several elements, such as Cu, Mg and Ag [3, 6–8], to modify the precipitation kinetics with forming phases (θ'-Al$_2$Cu, T$_1$-Al$_2$CuLi, S-Al$_2$CuMg), some of them in competition with δ' and δ, and enhance the mechanical properties.

δ' precipitation has been subject of intense study in the past years, in particular the coarsening behaviour [9–11]. Many studies have confirmed that coarsening of δ' precipitates follows the classical Lifshitz–Slyozov–Wagner theory of precipitate ripening [12, 13] with lithium diffusion through the lattice as the rate-controlling mechanism [9–11]. δ' precipitation process has been commonly studied in Al–Li alloys by non-isothermal measurements such as differential scanning calorimetry (DSC) [14, 15]. These works provide the activation energy of the precipitation process calculated by the so-called Kissinger method [16] but no further information of the kinetic reaction is given. However, as δ' precipitation proceeds via a nucleation and growth reaction, this reaction can be therefore analyzed my means of the classical kinetic models such as the Johnson–Mehl–Avrami–Kolmogorov (JMAK) and Austin–Rickett (AR) relations [17–21]. These models provide valuable understanding of the nucleation and growth processes, like the diffusion mechanism controlling the growth of precipitates [22], and have been successfully used in the

I. Gutiérrez-Urrutia (✉)
Max-Planck-Institut für Eisenforschung, Max-Planck Str. 1,
40237 Düsseldorf, Germany
e-mail: i.gutierrez@mpie.de

analysis of various precipitation reactions in aluminium alloys [23, 24]. Isothermal reactions allow a detailed analysis of precipitation kinetics from the direct fit of the data to the JMAK and AR relations. From these analyses kinetic parameters such as the so-called Avrami exponent can be calculated that provides significant understanding of the nucleation and growth process. The present study provides a detailed analysis of isothermal δ' precipitation kinetics in an Al–2.3 wt% Li–0.1 wt% Zr alloy obtained by the measurement of the thermoelectric power (TEP) in the temperature range between 120 and 180 °C. TEP was selected because of its high accuracy in the determination of variations in solute content [25, 26]. Precipitation kinetics were analyzed to the JMAK an AR relations. The values of kinetic parameters such as the Avrami exponent and the activation energy were calculated and discussed. The use of these relations to analyze precipitation reactions is discussed.

Experimental details

δ' precipitation kinetics at 120, 140, 160 and 180 °C were studied in an Al–2.3 wt% Li–0.1 wt% Zr alloy that was supplied by Alcan-Europe in the form of hot rolled plate. The thermoelectric power (TEP) measurements were performed at room temperature (20 °C) on a Techmetal instrument with an accuracy of ±0.002 μV/K. As reference metal, pure aluminium with mass close to that of the sample was used. To avoid any thermal gradient between the sample and the reference blocks, the TEP samples were machined to a convenient geometry of 50 mm in length with a cross-section less than 2 mm^2. The TEP samples were solution heat treated at 530 °C for 20 min followed by cold water quenching and subsequently stored in liquid nitrogen to minimize any precipitation effect at room temperature. Ageing treatments were performed at 120, 140, 160 and 180 °C, and finished by a quench into water at room temperature. δ' precipitation kinetics were examined by transmission electron microscopy (TEM) in a Philips CM200 transmission electron microscope operating at 200 kV. Thin foils were prepared using a twin-jet electropolisher with 25% nitric acid in methanol mixture operating at −25 °C.

Analysis of isothermal kinetics

Physical background of the TEP measurement

The principle of the thermoelectric power (TEP) measurement is based on the Seebeck effect. If a metal sample is subjected to a temperature gradient ΔT, then a voltage difference ΔV is generated across the sample due to the Seebeck effect. For a low thermal gradient, it holds: $\Delta V = \Delta S \cdot \Delta T$, where ΔS (Seebeck coefficient) is the difference between the TEP of the sample (ΔS_t) and the TEP of the reference metal (ΔS_0).

The precipitation kinetics are characterized by the evolution of ΔS with aging time. ΔS is affected by different types of lattice defects, such as solute atoms and precipitates, which are likely to modify the electronic or elastic properties of the matrix. The evolution of ΔS with aging time is governed by two effects [25, 27]. The first effect is attributed to the gradual decrease of the solute content as precipitation proceeds. This is determined by the specific TEP of the solute atom in the matrix (lithium in aluminium in the present alloy). This contribution is generally divided into two terms: a diffusion component and a phonon drag component. The first term is usually taken as a linear function of temperature and includes the solute content. The second term depends on the electron and phonon scattering processes. Solute atoms can have a positive or negative influence on the TEP of the matrix. In particular, it is known that solutes increase the TEP of aluminium if they precede this metal in the periodic table of elements [25]. The second effect is ascribed to the intrinsic effect of the precipitates formed during aging. This effect depends on the volume fraction, type, size and morphology of the precipitates [25, 27]. It has been reported that a low volume fraction (below 10%) of coarse incoherent precipitates in an aluminium alloy has a negligible influence on the TEP whereas coherent and semi-coherent precipitates may have a strong intrinsic effect on the TEP of the alloy. This result has been explained in terms of Bragg scattering of electrons by coherent particles [28].

Kinetic models

The analysis of reactions which proceed via nucleation and growth, such as precipitation reactions in aluminium alloys, is commonly performed by means of the JMAK and AR relations [22–24]. Although the original works focused on isothermal reactions [17–21], a considerable effort has been put forth in recent years to extend these relations to the analysis of non-isothermal reactions [23, 29–31]. As these relations are used in the present analysis, a brief description of these models is given here focusing on kinetic parameters.

The JMAK model makes use of the so-called 'extended volume' concept where the individual nuclei grow without any limitation of space. For diffusion-controlled precipitation reactions, the volume V of the region transformed at time t which nucleated at an earlier time r is defined as the volume of an imaginary fully depleted area around a precipitate needed to give a precipitate size equal to the

real case with a diffusion zone. The volume V is written as:

$$V = A\,[G(t-r)]^m \qquad (1)$$

where $G(t-r)$ is the growth rate, A is a constant related to the initial supersaturation, the dimensionality of the growth and the mode of transformation, and m is a constant related to the dimensionality of the growth and the mode of transformation. From relation (1) the extended volume of the precipitates which nucleated during the time interval $(r, r+dr)$ is written as:

$$dV_{ext} = A\,N(r)\,V_0[G\,(t-r)]^m dr \qquad (2)$$

where $N(r)$ is the nucleation rate and V_0 is the initial volume. Assuming that both the nucleation and growth processes are thermally activated, then an Arrhenius-type relation for both the nucleation $N(T)$ and growth rate $G(T)$ can be considered as follows [29, 31]:

$$N(T) = N_0\,\exp\left(-\frac{Q_N}{k_B T}\right)$$
$$\qquad (3)$$
$$G(T) = G_0\,\exp\left(-\frac{Q_G}{k_B T}\right)$$

where k_B is the Boltzmann constant, N_0 and G_0 are constants, and Q_N and Q_G are the activation energies associated to nucleation and growth process, respectively. Integrating Eq. 2 over the time and introducing $f(t) = V_{ext}/V_0$ as the transformed fraction, the following relation is obtained:

$$f(t) = 1 - e^{-k(T)\,t^n} \qquad (4)$$

where n is a constant, referred to as the Avrami exponent, and $k(T)$ is a temperature-dependent factor, which is usually taken as:

$$k(T) = k_0\,\exp\left(-\frac{Q}{k_B T}\right) \qquad (5)$$

where k_0 is a constant, k_B is the Boltzmann constant and Q is the activation energy associated to the transformation process. The Avrami exponent n is given as [22, 29, 31]:

$$n = ab + c \qquad (6)$$

and the activation energy associated to the transformation process Q is defined as:

$$Q = ab\,Q_N + c\,Q_G \qquad (7)$$

This relation shows that the activation energy Q can be expressed as a linear combination of the activation energies associated to nucleation and growth processes. The parameters a, b and c are related to the nucleation and growth processes as follows [22–24, 29, 31]. The parameter a is the dimensionality of the growth (1, 2 or

3). The parameter b is related to the type of growth. It takes 1 for interface-controlled growth and 1/2 for diffusion-controlled growth. The parameter c is related to the type of nucleation rate. In isothermal paths it takes 0 for site saturation (nuclei are present before the start of the transformation), 1 for continuous nucleation (constant nucleation rate), between 0 and 1 for decreasing nucleation rate, and higher than 1 for autocatalytic nucleation processes where the presence of nuclei enhances the formation of new nuclei.

The AR relation [18] is a phenomenological equation that has been used to analyze nucleation and growth reactions like bainite formation in shape-memory alloys [32] and precipitation reactions in aluminium alloys [23]. In this relation the transformed fraction $f(t)$ as a function of time t is written as:

$$\frac{f(t)}{1-f(t)} = k(T)\,t^n \qquad (8)$$

where n is the Avrami exponent and $k(T)$ the temperature-dependent factor. These kinetic parameters have the same meaning than those in the JMAK relation.

Results and discussion

Figure 1 shows the variation with time of the thermoelectric power (TEP) difference (ΔTEP) between the Al–2.3 wt% Li–0.1 wt% Zr alloy aged at 120, 140, 160 and 180 °C and pure aluminium. All the curves have the same appearance with three TEP stages clearly distinguishable. In the first stage ΔTEP is almost constant. This is a short stage that stands between 100 and 2,000 s depending on the aging temperature. In the second stage, ΔTEP diminishes steadily until the onset of the third stage where the decrease in ΔTEP is less significant. The observed ΔTEP variation in the present study is similar to that observed in resistivity measurements in Al–Li alloys, which is ascribed to δ' (Al$_3$Li) precipitation process [33–35]. δ' precipitation was confirmed in the present study by transmission electron microscopy (TEM). Figure 2 shows a dark-field TEM image using a δ' reflection of the Al–2.3 wt% Li–0.1 wt% Zr alloy aged at 180 °C for 900 s. This aging time corresponds to approximately the half of the second ΔTEP stage (Fig. 1). The microstructure consists of a homogeneous distribution of δ'(Al$_3$Li) precipitates with an average size of 40 nm and some few 'composite' precipitates Al$_3$(Li, Zr) (area fraction less than 0.1%) with an average size of 100 nm consisting of a core of Zr-rich particles surrounded by a shell of Al$_3$Li. It is well known that the addition of Zr to Al–Li alloys leads to the precipitation of an Al$_3$Zr or Al$_3$(Zr, Li) phase with the same crystallographic structure as the δ' phase. This promotes the heterogeneous
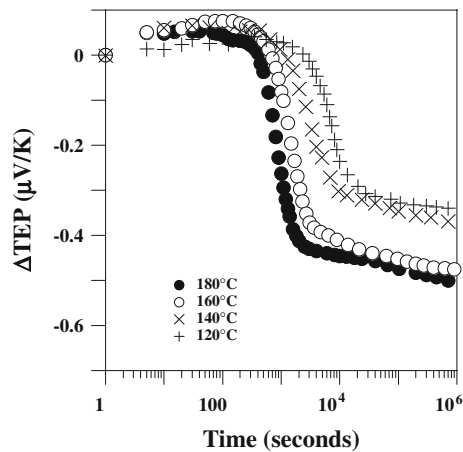
Fig. 1 Thermoelectric power difference (ΔTEP) variation with time in an Al–2.3 wt% Li–0.1 wt% Zr alloy aged at 120, 140, 160 and 180 °C
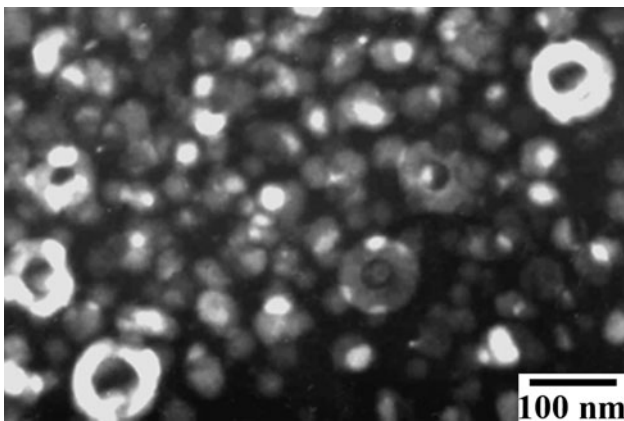

Fig. 2 Dark-field transmission electron image of the Al–2.3 wt% Li–0.1 wt% Zr alloy aged at 180 °C for 900 s. The precipitation distribution consists of δ' (Al$_3$Li) precipitates and composite particles (Al$_3$(Li, Zr)). The dark-field image was obtained using a δ' superlattice reflection

nucleation of the δ' phase on these particles resulting in the formation of the so-called 'composite' precipitates [36, 37]. δ (AlLi) phase was not observed during precipitation kinetics. This result agrees with previous observations on similar binary Al–Li alloys [9, 34].

The TEP variation of the present alloy is ascribed to the variation of lithium in solid solution and the presence of coherent δ' precipitates. Although the specific TEP of lithium in aluminium is unknown, we assume that it is positive according to the TEP values of different solutes in aluminium [25, 27]. Accordingly, a decrease of lithium in solid solution leads to a decrease in the TEP of the alloy. The effect of coherent δ' precipitates in the TEP of the alloy is expected to be positive, according to the model of Bragg scattering of electrons by coherent particles [28].

This model also estimates a decrease in the positive contribution of coherent particles to the TEP of the alloy with the coarsening of precipitates.

From the present results and previous studies on precipitation reactions in binary Al–Li alloys obtained by resistivity measurements [33–35], we provide the following interpretation of the TEP variation with time in the present Al–2.3 wt% Li–0.1 wt% Zr alloy. The first TEP stage is associated to the early stage of δ' formation (ordered domains). The positive value of ΔTEP in the first stage can be attributed to the formation of coherent δ' phases (early ordered domains) and the limited decrease of lithium in solid solution. In this stage, the contribution of ordered δ' domains to the TEP of the alloy is more significant than that provided by the solid solution variation. The second TEP stage is ascribed to δ' precipitation followed by the coarsening of the precipitates, identified as the third TEP stage. The decrease of ΔTEP in the second stage is ascribed to the removal of lithium from solid solution during δ' precipitation. The gradual decrease of lithium in solid solution during precipitate coarsening and the positive contribution (and probably small due to particle coarsening) of coherent δ' precipitates to the TEP of the alloy results in a limited decrease of ΔTEP. Coarsening of δ' precipitates is mainly attributed to the growing of particles by the impingement and coalescence of growing particles. This process does not involve any lithium removal from the matrix. It can be also seen that the TEP decrease associated to the second stage is much larger in samples aged at 160 and 180 °C than in samples aged at 120 and 140 °C (0.4 vs. 0.3 μV/K). This is related to the larger volume fraction of δ' precipitated in the high temperature range 160–180 °C.

δ' precipitation kinetics were analyzed by means of the JMAK and AR relations. We have assumed that ΔTEP is proportional to the transformed fraction $f(t)$ because the variation in the amount of lithium interchanged between one and another phase is small. Figures 3 and 4 show the fit of δ' precipitation kinetics to the JMAK and AR relations, respectively. It can be seen that both relations provide a good fit of the data well up to the third TEP stage, namely up to a transformed fraction of around 0.9. Above this fraction, third TEP stage, both fits deviate significantly from the kinetics data. Deviations from the JMAK relation have been reported in several reactions such as non-uniform transformations, transformations with anisotropic growth or transient nucleation [38–41]. In the present study the deviation is produced by the coarsening of δ' precipitates. Figure 5 shows a dark-field TEM image using a δ' reflection of the Al–2.3 wt% Li–0.1 wt% Zr alloy aged at 180 °C for 9000 s corresponding to a transformed fraction of 0.9. This figure reveals that at this stage the coarsening of δ' precipitates is noticeable.
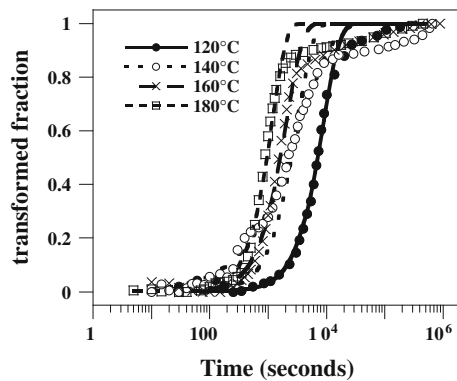
Fig. 3 Transformed fraction of δ′ (Al₃Li) precipitates in an Al–2.3 wt% Li–0.1 wt% Zr alloy at aging temperatures of 120, 140, 160 and 180 °C. Experimental data (*dots*) and fit to the Johnson–Mehl–Avrami–Kolmogorov (JMAK) relation (*lines*)
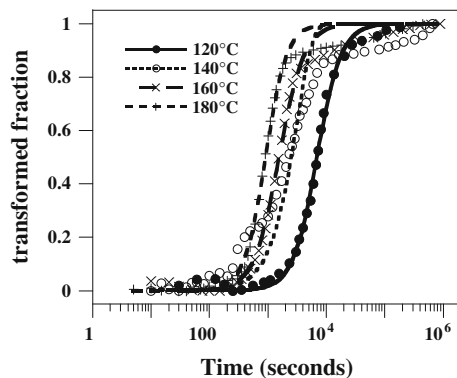

Fig. 4 Transformed fraction of δ′ (Al₃Li) precipitates in an Al–2.3 wt% Li–0.1 wt% Zr alloy at aging temperatures of 120, 140, 160 and 180 °C. Experimental data (*dots*) and fit to the Austin–Rickett (AR) relation (*lines*)
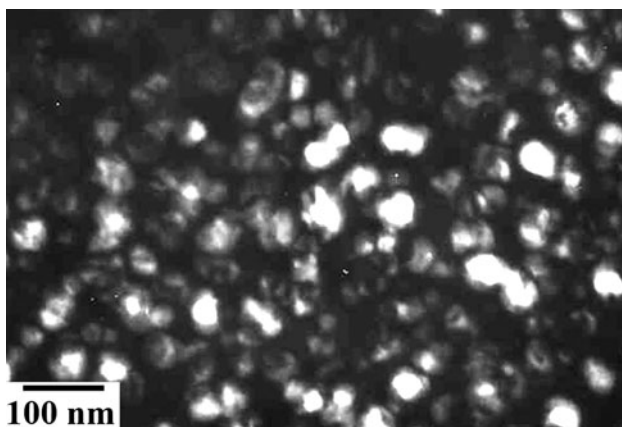

Fig. 5 Dark-field transmission electron image of the Al–2.3 wt% Li–0.1 wt% Zr alloy aged at 180 °C for 9000 s showing the coarsening of δ′ precipitates. The dark-field image was obtained using a δ′ superlattice reflection

δ′ precipitation process is characterized by two stages. The first stage is ascribed to a nucleation-and-growth mechanism. The second stage involves the coarsening of precipitate particles driven by the reduction in the total interfacial energies between precipitates and matrix. The present results show that the first stage is well described by the JMAK and AR relations whereas both relations fail to fit the second stage. This deviation is related to the impingement effect of growing precipitates. As currently there is no clear understanding of the impingement effect described by the AR relation, although in the past years some attempts have been made to describe this effect given on a physical ground [23, 32, 41], the discussion is only focused on the JMAK relation. This relation represents an idealized case where impingement of objects other than neighbouring precipitates is negligible. It ignores the fact that the growth of precipitates slows down before the physical interaction between precipitates takes place due to the saturation of untransformed regions with the elements diffusing away from the interface. In this sense the JMAK relation underestimates the impingement effect. Hence, the approximation can be expected to hold only for limited transformed fractions (in the present Al–Li alloy it holds up to a transformed fraction of around 0.9).

Accordingly, the following analysis of precipitation kinetics is restricted to the nucleation-and-growth stage. Two kinetic parameters are obtained from the fit of the data to both relations: the activation energy associated to the precipitation process and the Avrami exponent. The activation energy is obtained from relation (5) after plotting $\ln k$ vs. $1/T$. According to this relation, the slope of the straight line corresponds to $-Q/k_B$ where k_B is the Boltzmann constant. Figure 6 shows this plot for the data fitted to JMAK and AR relations. It can be seen that both relations provide the same value of the activation energy, 52 ± 1 kJ/mol. This value is significantly lower than the reported activation energy for volume diffusion of lithium in aluminium (140 kJ/mol [42]) but it is in the range of activation energies of migration of vacancies in aluminium alloys (45–65 kJ/mol [43]). This suggests that δ′ precipitation process in the present Al–2.3 wt% Li–0.1 wt% Zr alloy is controlled by the presence of excess vacancies quenched-in from the ageing temperature. In Al–Li alloys a large amount of quenched-in vacancies can be trapped during a certain time at or near δ′ precipitates preventing from being annealed out due to the high vacancy-lithium binding energy (25 kJ/mol [43]) [44]. As the activation energy for volume diffusion can be considered as the sum of the contributions due to formation and migration of a vacancy, the high concentration of excess vacancies yields a significant reduction of the activation energy resulting in a value close to the activation energy for migration of a vacancy. This effect has been also reported in previous
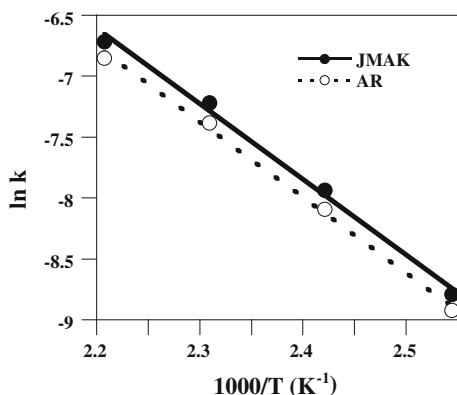
Fig. 6 Arrhenius plot of the activation energy for δ' (Al₃Li) precipitation in an Al–2.3 wt% Li–0.1 wt% Zr alloy for the fit to the Johnson–Mehl–Avrami–Kolmogorov (JMAK) relation (*solid line*) and the Austin–Rickett (AR) relation (*dashed line*)

Table 1 Avrami exponent n calculated from the fit of δ' (Al₃Li) precipitation kinetics obtained by the measurement of the thermo-electric power (TEP) to the Johnson–Mehl–Avrami–Kolmogorov (JMAK) and Austin–Rickett (AR) relations for an Al–2.3 wt% Li–0.1 wt% Zr alloy aged at 120, 140, 160 and 180 °C

Temperature	120 °C	140 °C	160 °C	180 °C
JMAK	1.55	1.50	1.53	1.65
AR	2.11	2.05	2.03	2.40

studies on precipitation reactions analyzed by differential scanning calorimetry (DSC) in aluminium alloys [44–46].

It is worth to compare the activation energy for δ' precipitation obtained in the present study by the measurement of the TEP with that obtained by other experimental techniques in similar binary Al–Li alloys. The present value of 52 kJ/mol is lower than that obtained by DSC measurements (87 kJ/mol [14]) or from the analysis of the kinetics of δ' coarsening by TEM or small-angle X-ray scattering (SAXS) (ranged between 76 and 134 kJ/mol [9]). Remarkably, most of the activation energies reported are lower than the activation energy for volume diffusion of lithium in aluminium (140 kJ/mol [42]). As δ' precipitation is extremely sensitive to the amount of quenched-in vacancies present in the matrix, the activation energy experimentally calculated in binary Al–Li alloys is ranged between the migration energy of a vacancy in aluminium (45–65 kJ/mol [43]) and the sum of the formation and migration energies of a vacancy, namely it is ranged between 45 and 140 kJ/mol. The amount of excess vacancies controlling the precipitation process and hence, the activation energy is determined by the experimental conditions. In the measurement of the TEP the sample is subjected to several cycles of aging and quenching (one cycle per experimental point with an overall of around 100). As excess vacancies are created after quenching, a large amount of vacancies can be continuously created during the measurement of the TEP enhancing δ' precipitation. However, the experimental conditions used in techniques such as DSC, TEM and SAXS to analyze δ' precipitation process are different to that used in the measurement of the TEP. In these techniques the sample is subjected to only two quenches: the first quench is performed after the solid solution heat treatment and the second quench after the corresponding ageing treatment. Consequently, the amount of quenched-in vacancies

created during the precipitation process is much lower than that produced in the TEP measurement, and therefore, the activation energy is larger. This result clearly shows that the experimental conditions play a key role on the determination of the activation energy of phenomena strongly dependent on vacancy content, such as δ' (Al₃Li) precipitation in Al–Li alloys, and therefore, attention must be paid on the interpretation of the corresponding reaction. In the present study, the experimental conditions inherent to the measurement of the TEP results into a precipitation process merely controlled by the vacancy migration energy in aluminium.

Table 1 shows the values of the Avrami exponent obtained from the fit of the kinetic data to the JMAK and AR relations. The JMAK relation provides an Avrami exponent ranged between 1.5 and 1.65 whereas the AR relation provides a larger value, ranged between 2.0 and 2.40. According to relation (6), these values correspond to a three-dimensional ($a = 3$) diffusion-controlled growth ($b = 1/2$) of a number of nuclei which is fixed at the beginning of the reaction, i.e. site saturation ($c = 0$, JMAK relation), or increases with a decreasing rate ($c < 1$, AR relation). It can be seen that both relations provide the same type of growth, which is consistent with the TEM image of Fig. 2. The only difference relies on the description of the nucleation process occurring during δ' precipitation. For the present isothermal conditions a site-saturation nucleation is more consistent than a nucleation with constant or variable nucleation rate [22, 47]. This implies that in the present Al–2.3 wt% Li–0.1 wt% Zr alloy, the JMAK relation provides a more convenient description of the δ' precipitation process than the AR relation. This is an interesting result because it suggests that the impingement effect in δ' precipitation can be well described by the JMAK relation until the last stage of the precipitation process where precipitate coarsening is significant. In the JMAK relation the impingement of growing nuclei is considered by means of the extended volume concept described above, i.e. the individual nuclei grow without any limitation of space. This result is contrary to that found in previous studies on precipitation reactions in aluminium alloys showing that the AR relation provides a better fit than the JMAK relation [23, 48]. In particular, Starink [23]

after analyzing several reaction processes claims that the AR relation is more appropriate in analyzing diffusion-controlled precipitation reactions than the JMAK relation. However, although in the past years some attempts have been made to describe the impingement effect given by the AR relation on a physical ground [23, 32, 41], at moment no clear description has been finally obtained. For this reason, the AR relation can be considered as a merely phenomenological relation whereas the JMAK relation provides a full description of the kinetic process. Deviations from the JMAK relation are expected due to its simple formulation, as reported in several works [38–40]. However, in order to consider further effects on the JMAK relation, such as precipitation coarsening, different approaches must be used, as a new formulation of the kinetic relation or even computer simulations [10, 49].

Conclusions

Isothermal δ' (Al$_3$Li) precipitation in an Al–2.3 wt% Li–0.1 wt% Zr alloy has been studied in the temperature range between 120 and 180 °C by the measurement of the thermoelectric power and transmission electron microscopy. The present study shows that the nucleation-and-growth stage of δ' (Al$_3$Li) precipitation reaction can be well described by the JMAK relation. The activation energy associated to the nucleation-and-growth stage calculated from the JMAK fit is 52 kJ/mol. The small activation energy obtained is ascribed to the presence of a large amount of excess vacancies quenched-in from the ageing temperature and inherent to the experimental conditions of the measurement of the TEP. This reduces the activation energy to a value close to the vacancy migration energy in aluminium (45–65 kJ/mol). The Avrami exponent associated to the nucleation-and-growth stage ranges between 1.5 and 1.65. These kinetic parameters indicate that δ' particles grow via a three-dimensional vacancy migration-controlled mechanism.

References

1. Martin JW (1988) Annu Rev Mater Res 18:101
2. Williams JC, Starke EA (2003) Acta Mater 51:5775
3. Csontos AA, Starke EA (2005) Int J Plast 21:1097
4. Nembach E (2000) Prog Mater Sci 45:275
5. Satya Prasad K, Mukhopadhyay AK, Gokhale AA, Banerjee D, Goel DB (1994) Scripta Metall 30:1299
6. Warner T (2006) Mater Sci Forum 519–521:1271
7. Lequeu P, Smith KP, Daniélou A (2010) J Mater Eng Perform 19:841
8. Steglich D, Wafai H, Besson J (2010) Eng Fract Mech 77:3501
9. Noble B, Bray SE (1999) Philos Mag A 79:859
10. Poduri R, Chen LQ (1998) Acta Mater 46:3915
11. Tsao CS, Chen CY, Kuo TY, Lin TL, Yu MS (2003) Mater Sci Eng A 363:228
12. Lifshitz IM, Slyozov VV (1961) J Phys Chem Solids 19:35
13. Wagner C (1961) Z Elektrochem 65:581
14. Noble B, Trowsdale AJ (1995) Scripta Metall Mater 33:33
15. Starink MJ, Gregson PJ (1996) Mater Sci Eng A 211:54
16. Kissinger HE (1957) Anal Chem 29:1702
17. Kolmogorov AN (1937) Ivz Akad Nauk SSSR, Ser Mat 3:355
18. Austin JB, Rickett RL (1939) Trans Am Inst Met Eng 135:396
19. Johnson WA, Mehl RF (1939) Trans Am Inst Met Eng 135:416
20. Avrami M (1939) J Chem Phys 7:1103
21. Avrami M (1940) J Chem Phys 8:212
22. Christian JW (1981) The theory of transformations in metals and alloys. Part I: equilibrium and general kinetics theory, vol 1. Pergamon Press, Oxford, UK
23. Starink MJ (1997) J Mater Sci 32:4061. doi:10.1023/A:1018649823542
24. Starink MJ, Zahra AM (1999) J Mater Sci 34:1117. doi:10.1023/A:1004516600251
25. Pelletier JM, Borrelly R (1982) Mater Sci Eng 55:191
26. Massardier V, Epicier T, Merle P (2000) Acta Mater 48:2911
27. Pelletier JM, Vigier G, Merlin J, Merle P, Fouquet R, Borrelly R (1984) Acta Metall 32:1069
28. Raynaud GM, Guyot P (1988) Acta Metall 36:143
29. Woldt E (1992) J Phys Chem Solids 53:521
30. Starink MJ (1997) J Mater Sci 32:6505. doi:10.1023/A:1018655026036
31. Ruitenberg G, Woldt E, Petford-Long AK (2001) Thermochim Acta 378:97
32. Lee ES, Kim YG (1990) Acta Metall 38:1669
33. Noble B, Thompson GE (1971) J Met Sci 5:114
34. Noble B, Harris SJ, Dinsdale K (1997) Acta Mater 45:2069
35. Noble B, Bray SE (1998) Acta Metall 46:6163
36. Gayle FW, Sande JBV (1984) Scripta Metall 18:473
37. Vecchio KS, Williams DB (1987) Acta Metall 35:2959
38. Sun NX, Liu XD, Lu K (1996) Scripta Mater 34:1201
39. Weinberg MC, Birnie DP, Shneidman VA (1997) J Non-Cryst Solids 219:89
40. Todinov MT (2000) Acta Mater 48:4217
41. Starink MJ (2001) J Mater Sci 36:4433. doi:10.1023/A:1017974517877
42. Costas LP, Marshall RP (1962) Trans Metall Soc AIME 224:970
43. Ceresara S, Giarda A, Sanchez A (1977) Philos Mag 35:97
44. Flower HM, Gregson PJ (1987) Mater Sci Technol 3:81
45. Rooyen MV, Mittemeijer EJ (1989) Metall Trans A 20:1207
46. Noble B, Trowsdale AJ (1995) Philos Mag A 71(6):1345
47. Starink MJ, Wang P, Sinclair I, Gregson PJ (1999) Acta Mater 47:3841
48. Starink MJ, Zahra AM (1998) Acta Mater 46:3381
49. Wang KG, Glicksman ME, Rajan K (2005) Comput Mater Sci 34:235